January, 1988] © *1988 The Chemical Society of Japan* *Bull. Chem. Soc. Jpn., 61, 59—69 (1988)* 59

Invited Paper

Pentaamminechromium(III) t_{2g}^3 Level Properties as Determined from Vibronic Spectra and Crystal Field Calculations

Hans-Herbert SCHMIDTKE,* Heribert ADAMSKY, and Thomas SCHÖNHERR
Institut für Theoretische Chemie der Universität Düsseldorf, D-4000 Düsseldorf 1, F.R.G.

(Received August 7, 1987)

Low temperature (~5 K) absorption and emission spectra of various halogenopentaamminechromium(III) salts have been recorded at high sensitivity in the intercombination region from pure microcrystalline powders and doped into corresponding rhodium complexes. Zero phonon and vibrational side bands are better resolved than reported in earlier investigations. They depend on the crystal lattice and allow a more detailed analysis of the vibrational fine structure. For carrying out reliable assignments to vibronic energy levels, the influence of the crystalline environment in different salts is found to be of major importance. Ligand field and angular overlap calculations are very helpful for solving the assignment problem, they can reproduce the proposed energy level scheme if symmetry adapted π-orbital expansion coefficients are introduced into the electron repulsion terms.

Since the pioneering work of A. E. Becquerel¹⁾ who reported the luminescence lifetime of ruby in 1867, chromium(III) ion lattices and complexes have become the subject of increasing research activity in the field of photophysics and photochemistry. In particular, the theoretical work of Tanabe and Sugano²⁾ has greatly stimulated the understanding of processes which are connected with light absorption and emission of these systems. At present, the discovery of the room temperature tunable alexandrite laser³⁾ and the potential use of chromium(III) doped glass ceramics as solar concentrators⁴,⁵⁾ have additionally focused attention on electronic and vibrational properties of d^3 complexes. Whereas, in general, most of the properties of ionic systems are determined by their particular lattices formed on crystallization, common coordination compounds as $[Cr(NH_3)_6]^{3+}$ or $Cr(acac)_3$ are better described by isolated molecular species in the solid using theoretical methods which are appropriate for investigating chemical bondings.⁶,⁷⁾ For examining the photochemical reaction pathways, starting from the optical spectra as a basis, in the past twenty years predominantly chromium ammine compounds have been extensively used as sample cases.⁸,⁹⁾

In an early attempt, Schläfer¹⁰⁾ related the energy gap between the ^2E_g and $^4T_{2g}$ levels (in O_h notation) derived from spectroscopically obtained ligand field (LF) parameters to the type of photophysical activity (fluorescence or phosphorescence), an observation which later has been named as Schläfer's rule. In an alternative point of view, the various ways of metal–ligand bonding have been considered for rationalizing the experimental results by classifying the ligands according to their extent of σ- and π-interactions towards the central metal.¹¹⁾ More recently, this idea has been taken over for use in the angular overlap model (AOM) by which photosubstitution processes could be investigated calculating metal–ligand strengths in the excited state.¹²⁾ Although this procedure seems to account for the majority of results obtained from low symmetry chromium(III) ammine complexes, the predictions on photosubstitution concerning the leaving group have been claimed to be incorrect for some of the acidopentaammines.¹³⁾ Forster and coworkers have examined the emission spectra of more than 40 tetragonal ammine complexes.¹⁴,¹⁵⁾ They classified these compounds, by inspection of band shapes obtained, into ^2E_g and $^2T_{1g}$ emitters and expressed the energies of the lowest excited states by AOM antibonding parameters derived from level splittings as measured for spin-allowed transitions into quartet states. In addition, the doublet transition energy has been found to be of major influence on the nonradiative decay rate, and even a slight modification of the second coordination sphere could lead to drastic changes of luminescence properties.¹⁶⁾ "Although a considerable body of data has been collected···the relative importance of changes in electronic and vibrational factors that accompany ligand substitution is not yet clear" (quoted from Ref. 17). Compared to the amount of experimental results reported in the literature, theoretical investigations on electronic states arising from t_{2g}^3 electron configuration are more rare. For instance, the magnitude of the splitting of the lowest excited ^2E_g level due to lower symmetry is not clear and has been an object of controversy;¹⁸⁻²⁰⁾ also information on the location of the spin-orbit split components of $^2T_{1g}$ and $^2T_{2g}$ is very scarce²¹⁾ and explanations for the in various complexes²²⁻²⁴⁾ anomalously large $^4A_{2g}$ ground state splitting is still unsatisfactory. On the other hand, since much of the experimental work cited above was performed on glassy solutions yielding poorly resolved spectra, the amount of information which can be obtained from these results is very limited.

Therefore, we want to report in the following some low temperature absorption and emission spectra of microcrystalline materials of pure halogenopentaammine complexes and doped in crystal lattices of similar composition yielding much better resolved band patterns as obtained earlier. The characterization of zero phonon bands different from vibrational side bands supplies an improved basis for carrying out band assignments and determining level splittings due to the lower symmetry; it contributes to investigate the role of spin-orbit coupling and covalent bonding effects on the energy level scheme and transition probabilities. Distortions of the nuclear framework in the excited state and, eventually, changes of potential energy surfaces close to the equilibrium geometry may be obtained from an analysis of the vibrational fine structure yielding evidence on the strength of vibronic coupling, important for the energy transfer and reactivity of the molecule. Parallel to the experiments various calculations have been carried out using common theoretical models as LF theory and the AOM, introducing only minor modifications when proved to be necessary. The results supply important contributions to the discussion of the assignment problem.

Experimental

Preparation of Compounds. The chromium(III) complexes were synthesized according to methods given in the literature.[25] The chloro- and bromopentaammine salts, abbreviated by $[Cl]Y_2$ and $[Br]Y_2$, were purified by metathesis from saturated solutions in respective acids HY. Preparation of iodopentaammine is interfered by rapid hydrolysis processes which prevent further recrystallization. The quality of these samples was checked by recording their luminescence spectra which are very sensitive to decomposition. Deuterated materials were obtained by repeated treatment of saturated D_2O solutions with DY. Small single crystals (0.2—0.5 mm diameter) of $[Cl]Cl_2$ were grown from hot (60 °C) acidified aqueous solutions within several hours. Analogous rhodium(III) compounds for use as suitable host crystals were prepared from $[Rh(NH_3)_5Cl]Cl_2$ which was recrystallized following given procedures.[26]

Spectroscopic Measurements. Visible and ultraviolet spectra were recorded using an appropriately modified Cary 17 spectrophotometer equipped with an RCA 4832 photomultiplier. Polarized spectra obtained from a specially designed microscopic optical device[27] gave additional information only on the splittings of the broad quartet bands. Absorption and emission spectra due to intercombination transitions were measured using a McPherson 0.5 m double monochromator model 285 fitted with a 1200 lines/mm grating and a red sensitive GaAs photomultiplier. For comparing peak intensities the emission spectra are corrected for apparative response. Further parts of the equipment have been an argon laser and a helium flow cryostat allowing temperature to be reached at the sample down to 5 K. Low excitation intensities were necessary to prevent photodecomposition of the compounds. The 20 K Raman spectrum of $[Cl](NO_3)_2$ was recorded by T. Woike[28] using the 620 nm line of an optically pumped dye laser. Under these mild conditions the spectrum can be reproducibly recorded avoiding photodecomposition to a large extent.

Energy Levels

Electronic States. Octahedral complex compounds of transition metal ions with t_{2g}^3 electron configuration have $\binom{6}{3}=20$ electronic levels which due to the molecular symmetry are in part degenerate leading to the multiplet states $^4A_{2g}$ (ground state), ^2E_g, $^2T_{1g}$, and $^2T_{2g}$. At lower symmetry these states are split into a maximum of 10 energy levels leaving a residual twofold degeneracy (Kramers doublets) if magnetic fields are absent. For C_{4v} point symmetry pertinent for the present compounds, the level symbols and level splittings due to the various interactions considered are indicated in Fig. 1.

Electron transitions between these states exhibit, at least for helium temperature spectra of crystalline solids, well resolved vibrational fine structure which can be compared to the IR and/or Raman spectra, vibrational quanta in the t_{2g}^3 excited states being similar to those in the ground state since chemical bonding will not be changed very much on excitation into levels arising from the same electron configuration. An analysis of the fine structure identifying particular vibrational side bands is, nevertheless, not easy because band superpositions will occur to a large extent due to several electron transitions being located close to each other. In particular, the positions of the low symmetry spin-orbit levels arising from $^2T_{1g}$ and $^2T_{2g}$ are difficult to localize in the energy level scheme

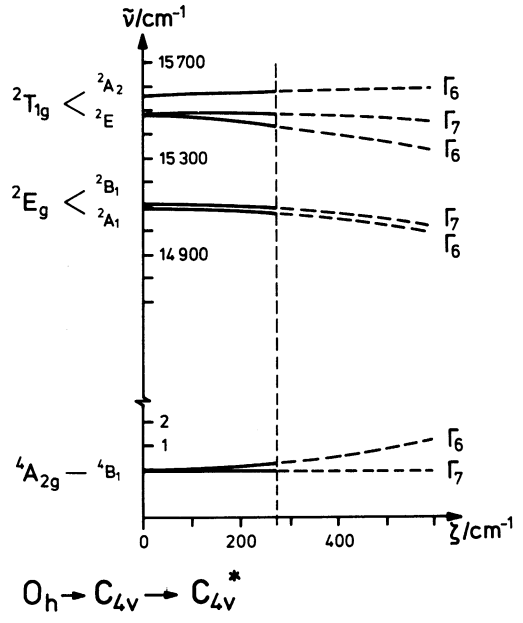

Fig. 1. Electronic t_{2g}^3 LF level scheme for C_{4v} symmetry chromium(III) complexes depending on the spin-orbit coupling coefficient ζ, for heavier ligands exceeding the parameter of the free ion (dotted lines). Model parameters chosen are $\sigma_N=7500$, $\pi_N=0$, $\sigma_X=5000$, $\pi_X=750$, $B=600$, $C=3500$, all in cm^{-1}.

(see below); as far as the first excited ^2E_g level is concerned a splitting between 20 cm^{-1} for [H_2O](ClO_4)$_3$ and about 200 cm^{-1} for halogenopentaammine complexes [X] have been reported.[18,19] The latter result cannot be reproduced by conventional LF calculations[18,20] although level schemes of similar mixed halogeno-amine complexes of Cr(III) are explained very well by applying this model.[29] A substantial increase of ^2E_g level splitting is, however, calculated when different nephelauxetic effects are assumed for $b_2(d_{xy})$ and $e(d_{xz},d_{yz})$ orbitals of C_{4v} symmetry (see below). Since no crystal structural data had been available, earlier calculations could not use actual molecular geometries. Recently, however, the room temperature crystal structure of [Cl]Cl_2 has been reported[30] according to which the chromium ions occupy equivalent sites with approximately C_{4v} symmetry. The exact site symmetry is only C_s and the space group $D_{2h}^{16}\equiv Pnma$.

By spin-orbit coupling the multiplet levels are split by different amounts (see Fig. 1), the $^4B_1(C_{4v})$ ground state splitting being very small which cannot be resolved by electronic spectroscopy. ESR results report zero field splittings of the ground state of some 0.2 (chloro complex) to 0.9 cm^{-1} (iodo complex).[22,31,32] The experimental splittings thus obtained for the heavier halogeno complexes turn out to be much larger than those predicted from conventional LF calculations from which it was concluded that the effective spin-orbit coupling constants should be increased to unusual high values.[22] To what extent this assumption can be justified will be discussed when describing the LF calculations.

Vibrational Levels. In the infrared spectrum only vibrations of a_1 and e symmetry type will be expected on the basis of C_{4v} selection rules, in the Raman spectrum on the other hand all vibrational transitions of CrN_5X chromophore are allowed. Figure 2 illustrates the 20 K Raman spectrum of [Cl](NO_3)$_2$ which due to the easy photodecomposition of the compound is only obtained by a careful wave length selection of incident light. Assignments to internal complex vibrations were made on the basis of available infrared data, normal coordinate analyses,[33]

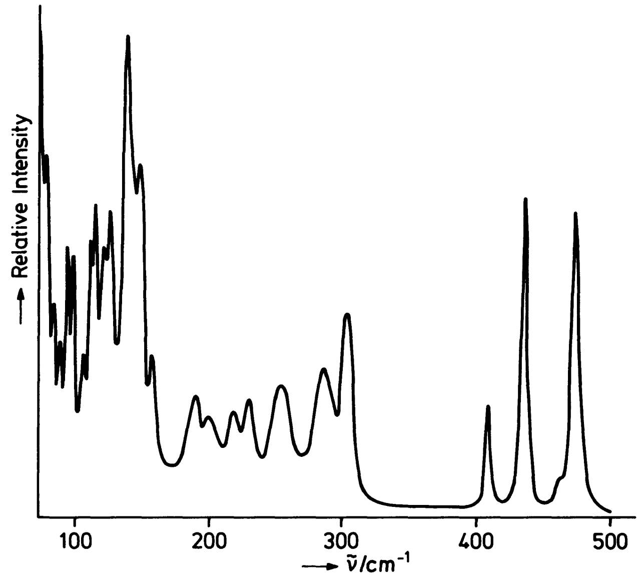

Fig. 2. Raman spectrum of [$Cr(NH_3)_5Cl$](NO_3)$_2$ at 20 K obtained from a 620 nm dye laser excitation.

Table 1. Normal Vibrations and Observed Frequencies for [Cl]Y_2 Compounds Obtained for Y=NO_3 from Raman and Emission Spectra and for Y=Cl from the Emission Spectrum only

No.	Symmetry	Atomic group vibrations (approximate)	Observed frequency[Cl]Y_2		ν(H)/ν(D)
			Y=NO_3	Y=Cl	Y=Cl
ν_1	a_1	$\sigma(Cr\text{-}NH_3)_{ax}$	471	477	1.06
ν_2	a_1		434	438	
ν_3	b_1	$\sigma(Cr\text{-}NH_3)_{eq}$	406	415	1.08
ν_4	e		460	465	
ν_5	a_1	σ(Cr-X)	301	309	1.02
ν_6	a_1		215	214	1.11
ν_7	b_1		189	187	1.08
ν_8	b_2	$\delta(H_3N\text{-}Cr\text{-}NH_3)$	285	276	1.11
ν_9	e		252	254	1.10
ν_{10}	e		125	115	1.10
ν_{11}	e	$\delta(H_3N\text{-}Cr\text{-}X)$	147	141	1.00
ν_{12}	a_1		805	806	1.30
ν_{13}	a_2		745	751	1.27
ν_{14}	b_1	$\delta(Cr\text{-}N\text{-}H)_{eq}$	660	667	1.30
ν_{15}	b_2		680	687	1.32
ν_{16}	e		766	771	1.28
ν_{17}	e		700	702	1.32
ν_{18}	e	$\delta(Cr\text{-}N\text{-}H)_{ax}$	—	652	1.31

and results obtained from the present vibronic spectra. Table 1 compiles all normal vibrations of given symmetry type involving the chromium central atom; also an assignment of all vibrational frequencies together with their deuterium shifts measured for the chloro complex is given.

Results and Discussion

^2E_g and $^2T_{1g}$ Spectrum. In Fig. 3 the crystalline powder absorption spectra of three halogenopentaammine complexes recorded at low temperature (~5 K) in the $^4A_{2g} \rightarrow {}^2E_g$, $^2T_{1g}$ (O_h notation) energy region are illustrated. The dominating band peaks indicated by A, B, and C are assigned in agreement with earlier works[18–20] to zero phonon transitions; on deuteration they exhibit isotope shifts which are negligible compared to the other bands. The vibronic side band pattern can be explained in terms of σ(Cr–NH$_3$), σ(Cr–X), δ(H$_3$N–Cr–NH$_3$), and δ(Cr–N–H) atomic group vibrations of the chromophore (cf. Table 1). Assignment of zero phonon peaks to their octahedral parent states ^2E_g and $^2T_{1g}$ is, however, in dispute[18–20] (see above).

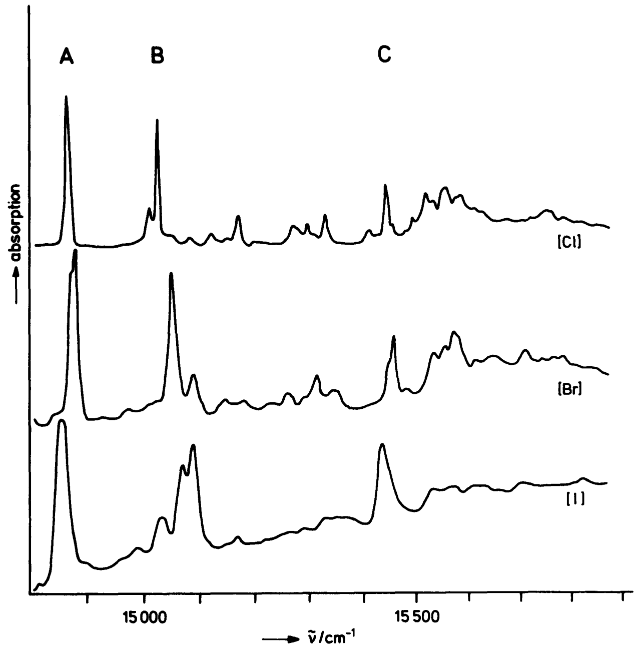

Fig. 3. Overall 5 K absorption spectra in the ^2E_g and $^2T_{1g}$ region of micro crystalline [Cr(NH$_3$)$_5$X]-(NO$_3$)$_2$.

The relative intensities of vibronic side bands obviously decrease in the series from [Cl] to [I] which may be explained by the larger perturbation of the octahedral symmetry by heavier halogen ligands breaking the d-d parity selection rule more efficiently and making pure electronic transitions allowed. It is further noticed that the band A belonging to the lowest transition energy is not much affected by the hetero ligands Cl, Br, or I which seems to be surprising in view of the fact that the energy gap to the ground state, approximately given by Racah parameters 9B+3C, ought to be subject to a varying nephelauxetic effect in this series of compounds. Also the energy difference between A and C peaks is almost unchanged in the spectra, only the position of the B bands varies to a certain amount. On the other hand crystalline effects are much larger than expected which becomes apparent from changing the anions of the salts, they even dominate the band shifts resulting from a variation of the hetero ligand (cf. Table 2).

$^2E_g(O_h)$ Splitting. The spectrum of crystalline [Cl]Cl$_2$ recorded with high resolution (better than 2 cm^{-1}) exhibits a splitting of the A band into two components A_I and A_{II} of different intensities (cf. Fig. 4). Half widths (8—10 cm^{-1}) and peak separations (12 cm^{-1}) are measured equally well for the deuterated complex (separation 14 cm^{-1}). In the emission spectrum the two peaks are found at almost identical frequencies, the intensity of the peak at higher energy increasing with temperature. For different counter ions the band profile changes, however, significantly. This applies for the degree of splitting and for the

Table 2. Zero Phonon Bands (in cm^{-1}) of [Cr(NH$_3$)$_5$X]Y$_2$ due to t_{2g}^3 Transitions Obtained from Low Temperature Absorption Spectra. I Refers to the Main Peak, II to a Satellite Peak or Shoulder

Compound	A_I	A_{II}–A_I	B–A_I	C_I–A_I	C_{II}–C_I
[Cl](NO$_3$)$_2$	14866	+6	160	580	—
[Cl]Cl$_2$	14826	−12	179	598	−7
[Cl]Br$_2$	14782	—[a]	188	589	—[a]
[Cl]I$_2$	14719	<0	192	617 (537)[b]	15 (−20)[b]
[Br](NO$_3$)$_2$	14888	−7	170	575	−9
[Br]Br$_2$	14780	−13	224	602	−10
[I](NO$_3$)$_2$	14853	+11	237	585	+10
[I]I$_2$	14656	—[a]	307	600	—[a]
Proposed Assignment:	$^2A_1(^2E_g)$		$^2B_1(^2E_g)$	$^2A_2(^2T_{1g})$	

a) Broad band, splitting not resolved. b) Alternative assignment possible.

relative intensities of the peaks as well (see Table 2) which may have different explanations depending on the assignment made to the low symmetry level scheme (see later). Ligand field theory using common model parameters predicts the transition into the $\Gamma_6(^2A_1)$ component (cf. Fig. 1) to be lowest in energy. In addition, for some of the complex salts, e.g. $[Cl](NO_3)_2$, in this zero phonon region another much weaker transition is detected which in the absorption spectrum is observed as a shoulder.

The corresponding doublet band patterns could not be resolved in the case of $[NCO](NO_3)_2$[20] and $[I]I_2$ (Table 2), on the other hand in the spectra of most of the compounds investigated two transitions are observed which are located closely together in energy, one (A_I) with a higher intensity than the other (A_{II}). It is tempting to assign these peaks to the C_{4v} symmetry splitting of $^2E_g(O_h)$, i.e. to $^2A_1$ and $^2B_1$ which would be in agreement with the assignment proposed for the $[H_2O]$ and $[OH]$ perchlorate.[19] However, pair interactions of paramagnetic Cr^{3+} centers could also give rise to additional peaks in the intercombination spectra.[34] Since these pair states are essentially determined by Cr–Cr distances we also investigated doped materials (0.1—3%Cr^{3+}) in corresponding Rh(III) complex salts. The spectra of these samples show, however, a quite similar A band pattern by which the occurrence of pair spectra can be excluded.

A further, more probable explanation is offered by the presence of different sites for Cr positions in the crystal. The space group *Pnma* obtained at room temperature for the $[Cl]Cl_2$ has only equivalent sites available for Cr atoms,[30] however, a temperature dependent X-ray investigation carried out on a powder sample distinctly reveals a structural phase transition between 220 and 230 K which cannot be detected in the electronic spectrum due to the lack of appropriate fine structure at these temperatures. Consequently we prefer to assign the band at A to only one of the ^2E_g split levels, the pair character being due to different sites; the other ^2E_g component then gives rise to the B band 150 to 300 cm^{-1} higher in energy. This interpretation would also explain the doublet structure of the zero phonon band C (cf. Table 2) although a similar pattern for B which equally well should be expected as a pair of bands could not be resolved. The varying band profile of A observed when changing the counter ion is then due to different environmental effects on crystalline Cr sites.

$^2T_{1g}(O_h)$ Splitting. From the six-fold degenerate $^2T_{1g}$ level which in octahedral complexes is located some 550 to 600 cm^{-1} higher than ^2E_g, at maximum three Kramers doublets can result (cf. Fig. 1) from which in tetragonal symmetry the $^2E(^2T_{1g})$ levels are appreciably decreased in energy due to interaction with the higher $^2E(^2T_{2g})$ levels of the same symmetry. The change in energy can be estimated from the AOM perturbation matrix by

$$\Delta E(^2E) = \frac{(\pi_L - \pi_X)^2}{6B + 2C} \tag{1}$$

with antibonding parameters π_L and π_X for the ligands L and X of a ML_5X chromophore. Since this expression is a negative contribution to the energy for any parameters associated to the ligands, $^2E(C_{4v})$ resulting from $^2T_{1g}(O_h)$ is always stabilized. On the other hand, the second $^2T_{1g}$ component, i.e. $^2A_2$, is almost unchanged on symmetry reduction since except for smaller spin-orbit coupling effects no interactions of neighboring levels are possible by symmetry reasons. As band C remains at almost equal position, e.g. in the series [Cl], [Br], and [I] of nitrate salts (see Table 2) for which π_X should essentially change, an assignment of this zero phonon band to $^2A_2$ seems to be straightforward (see crystal field calcula-

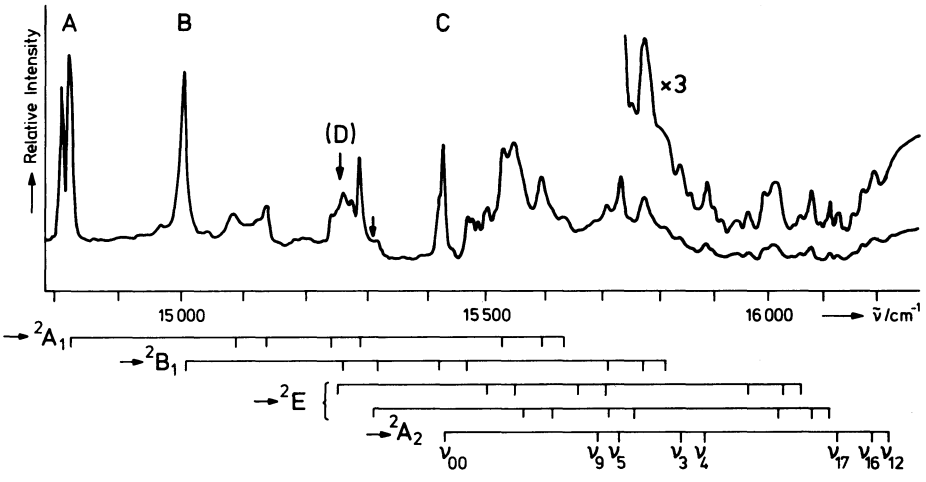

Fig. 4. High resolution absorption spectrum of $[Cr(NH_3)_5Cl]Cl_2$ at 5 K and vibronic assignments to C_{4v} symmetry levels (in the neighboring energy region narrow line spectra cannot be resolved).

tions).

Reliable assignments of $^4B_1 \rightarrow \Gamma_6, \Gamma_7(^2E)$ transitions in absorption spectra of low symmetry Cr(III) ammine complexes have not been carried out as yet because corresponding peaks are usually superimposed by vibrational side bands of $\Gamma_6(A_1)$ and $\Gamma_7(B_1)$ transitions arising from $^2E_g(O_h)$, the zero phonon peaks of which we have assigned to the A and B band. For localizing hidden zero phonon transitions in this region a vibronic band analysis must be performed assigning all vibronic intervals to normal vibrations known from Raman and luminescence spectra. In Fig. 4 the result of this analysis obtained for the $[Cl]Cl_2$ spectrum is presented by indicating the normal modes which give rise to absorption peaks in the side band spectrum. For this assignment only those vibrational quanta are used which are measured in the luminescence spectrum as main bands; by this virtually all satellite peaks can be explained. The same procedure is applied also to the corresponding deuterated compound which allows for checking each of the band assignments by regarding the expected isotope shifts of Table 1. As a result we conclude that a further zero phonon transition (D) should be present at 15246 cm^{-1} that is calculated from vibrational intervals belonging to ν_3, ν_5, ν_9, and ν_{16} to ν_{18} quanta. Indications for another zero phonon transition in this region also lower in energy than $^2A_2$ are found at a position marked by an arrow in Fig. 4 which could originate from the second split component of $^2E(C_{4v})$. However, these assignments are less certain.

$^2T_{2g}$ Spectrum. In Fig. 5 the spectrum of $[Br]Br_2$ is presented which includes also quartet transitions. Superimposed to one of these quartets the highest $t_{2g}{}^3$ intraconfigurational transitions can be detected with unusually large intensity. A similar band pattern has been reported[35] in this region for $tr[Cr\,en_2Br_2](ClO_4)$ which was explained being due to the D_{4h} components ^2E_g and $^2B_{2g}$ of $^2T_{2g}(O_h)$. Güdel and co-workers, on the other hand, have assigned two narrow band shoulders they detected on the short wave length flank of the first quartet band of $[OH](ClO_4)_2$ to the Γ_6 and Γ_7 components of $^2E(^2T_{2g})$, however, did not find any other fine structure close to these absorptions.[19] The present band profile obtained for $[Br]Br_2$ (similar features can be observed at high resolution also in the other halogenopentaammine spectra) with a relatively slowly decreasing progression of about 240 cm^{-1} is detected only at low temperatures. It cannot be assigned to a spin allowed transition, since quartet bands remain essentially unchanged on cooling to liquid helium temperatures. Higher intensities (extinction coefficients $\varepsilon \sim 10$) and larger band widths ($\sim 50\ cm^{-1}$) can be well explained from the interacting electronic energy level scheme considering spin-orbit coupling. Relevant finite off-diagonal perturbation matrix elements intermixing ^2E and $^4B_2$ wave functions of C_{4v} are

$$\langle \Gamma_6(^2E)\,|\,H_{SO}\,|\,\Gamma_6(^4B_2)\rangle = -\frac{\zeta}{2}$$
$$\langle \Gamma_7(^2E)\,|\,H_{SO}\,|\,\Gamma_7(^4B_2)\rangle = -\frac{\zeta}{\sqrt{12}} \tag{2}$$

ζ being the one-electron spin-orbit coupling coefficient, while the corresponding matrix element with the second $^2T_{2g}(O_h)$ component, i.e. $\Gamma_7(^2B_2)$, is vanishing.[36] Other interactions of this kind involving the $^4E(C_{4v})$ state of $^4T_{2g}$ are small due to the energy denominator which is several thousand wavenumbers larger than for interactions with $^4B_2(C_{4v})$. Due to the larger mixing coefficient of $\Gamma_6(^4B_2)$ into $\Gamma_6(^2E)$ functions the transition into the $\Gamma_6(^2E)$ state should

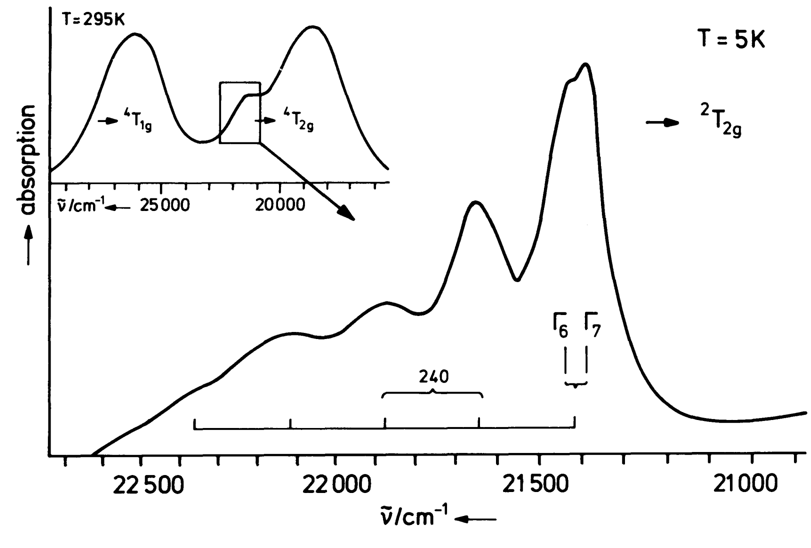

Fig. 5. Room temperature quartet absorption spectrum and 5 K high resolution $^2T_{2g}$ spectrum.

obtain higher intensity than for $\Gamma_7(^2E)$; the total splitting into Γ_6 and Γ_7 of ^2E is computed by a complete ligand field calculation to be some 50 cm^{-1} which is in good accordance with the assignment given in Fig. 5. The band widths, which are increased compared to usual doublet transitions of Cr(III), also indicate a higher contribution of quartet character which accounts for the occurrence of a vibrational progression due to larger nuclear distortions with respect to the ground state geometry.

The Fluoro Complex. In the series of halogenopentaammines of chromium(III) the fluoro complex spectrum obviously occupies a particular position. In the region of $^4A_{2g} \rightarrow {}^2E_g$ zero phonon transitions the absorption spectrum shows six intensive peaks, some with different half widths (cf. Fig. 6). In the emission spectrum corresponding bands are located at equal energies, their intensities being strongly temperature dependent which partly can be explained by Boltzmann distribution. The band pattern is repeated a few times shifted towards smaller wavenumbers into the vibrational side band region. These findings are best accounted for by the presence of a bunch of zero phonon transitions which arise from several nonequivalent sites in the crystal. Unfortunately no structural data is available for the fluoropentaamminechromium complex (as is not for other central metal ions). A preliminary powder X-ray recording at room temperature indicates a complicated super structure which is not unusual for perchlorate lattices. This would be in agreement with the given interpretation assuming nonequivalent chromium positions. A possible explanation may be given by the smaller size of the fluoride ion compared to NH_3 ligands preventing the hetero-ligand to favor a certain coordinate direction in the crystal lattice (the complex is considered to be built into the holes of the anion lattice) that would lead to a formation of different sites in the crystal.

An analysis of the vibrational side bands similar to the discussion carried out for the other halogeno complexes is not possible due to large band superpositions and a lack of sufficient peak resolution in this spectrum. Therefore also the zero phonon lines arising from $^2T_{1g}(O_h)$ split levels cannot be located. However, the slowly decreasing progressions in 530 cm^{-1} quanta clearly identified in the emission spectrum are explained being due to the metal-halogen stretching vibration $\nu_5(a_1)$ which is also observed in the spectra of the other pentaammine complexes. The intensity distribution in these progressions will be used for determining the geometric distortion of the emitting state (see below).

Crystal Field Calculations. Conventional LF and AOM calculations are, in general, able for the present compounds to account for the electronic energy level scheme verified from the experiment.[19,20,36] There are, however, some exceptions: e.g., the size of the low symmetry splitting of the $^4A_{2g}(O_h)$ ground and first excited state ^2E_g cannot be reproduced, i.e. in the experiment they are found about one order of magnitude larger than from theory even though when complete LF calculations are carried out considering all possible $\binom{10}{3}=120$ wave functions of the d^3 electron configuration. The highest level splittings calculated from usual model parameters which hold also for other chromium(III) complexes are ~0.3 cm^{-1} for $^4A_{2g}$ and ~50 cm^{-1} for ^2E_g. The results do not change very much if various improvements are implemented in the computer program:[21] consideration of the real

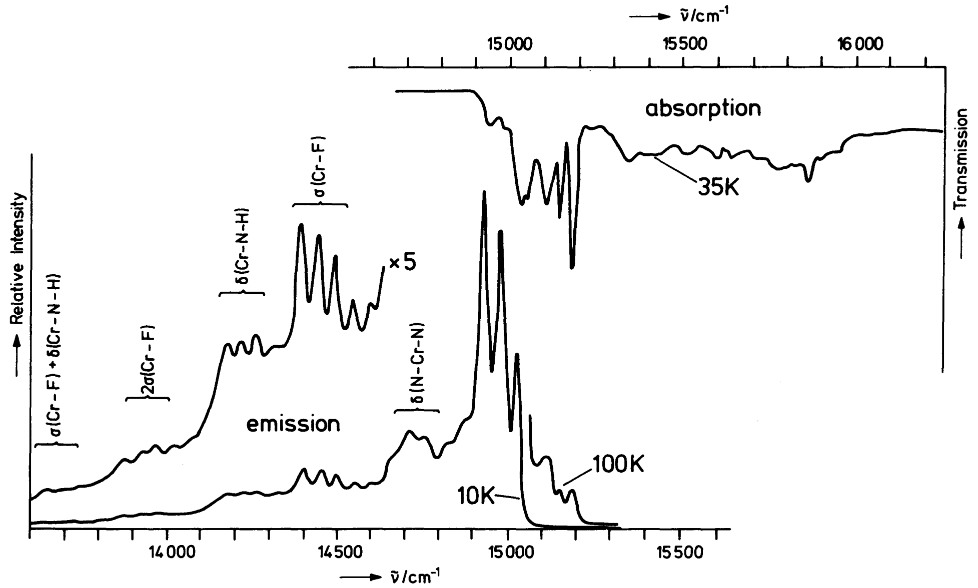

Fig. 6. Vibronic absorption spectrum (35 K) in the intercombination region and emission spectrum (10 K and 100 K, $\lambda_{exc}=514.5$ nm) of $[Cr(NH_3)_5F](ClO_4)_2$.

geometry, introduction of Trees correction, distinction of nephelauxetic effects for e_g and t_{2g} orbitals ($\beta_{55}\neq\beta_{35}\neq\beta_{33}$ according to Jørgensen[37]), and inclusion of potential interactions to the second coordination sphere by considering for hexacoordinated systems σ bonds between t_{2g} metal- and p-functions of the anions.[16] We have undertaken to check in detail all these influences by performing extensive ligand field calculations varying parameters within ranges being of physical significance which reproduce the correct quartet level sequences as derived from the polarized spectra, with the result that all these effects are not capable to explain the large ^2E_g splitting of these compounds. This is in agreement with earlier investigations.[16,18–20,36]

The incomplete treatment of the electron repulsion part that uses only parameters adapted to spherical symmetry has been criticized already earlier[18,37] and some founded extensions of the original models have been proposed to remove this shortcoming. A consequent consideration of electron repulsion leads, however, even at cubic symmetry to an inflation of parameters,[38] by which the convenient relations between theory and experiment, very useful in practice within the conventional models, are lost. The way out of this problem may be shown by the Stevens delocalization coefficients,[37] which in O_h symmetry consider differences in the LCAO expansion coefficients μ for e_g and t_{2g} orbitals,[39] i.e.

$$\psi = \mu\varphi_M + \lambda\varphi_L \tag{3}$$

At this symmetry only two sets of μ,λ-coefficients are possible. The neglect of more center integrals justified by the strong localization of d-orbitals on the metal atom leads to various electron repulsion terms differing in symmetry

$$\mu_a\mu_b\mu_c\mu_d\langle ab|1/r_{12}|cd\rangle \tag{4}$$

(each $\mu_i<1$) which can be expressed again by linear combinations of spherical Slater–Condon or Racah parameters.

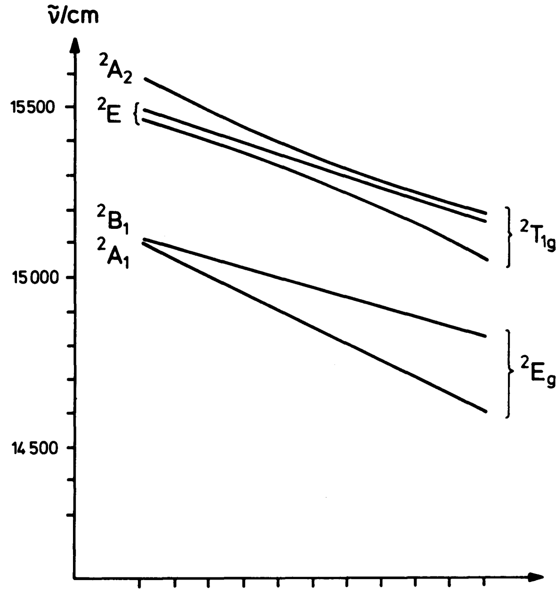

Fig. 7. Low symmetry ligand field splitting of ^2E_g, $^2T_{1g}$ levels depending on the π-orbital expansion factor τ (see text). Parameters are chosen as in Fig. 1 and $\zeta=200\,\text{cm}^{-1}$; $\varepsilon_u=\varepsilon_v=1.0$.

For C_{4v} complexes the corresponding symmetry adapted μ-coefficients may be denoted by τ_ζ of d_{xy}, $\tau_\xi=\tau_\eta$ of d_{yz}, $d_{xz}(t_{2g})$ and ε_u of $d_{x^2-y^2}$, ε_v of $d_{z^2}(e_g)$. Since NH_3 ligands do not contribute to π-bonding ($\pi_N=0$), for present pentaammine complexes the corresponding π-coefficient is $\tau_\zeta=1$. A complete AOM calculation performed with a significant set of parameters shows that already a very small deviation of the other τ parameters from unity has a large effect on the ^2E_g splitting (cf. Fig. 7), the size of the ε-expansion coefficients chosen for e_g orbitals is found to be of minor importance for the splitting pattern of ^2E_g and $^2T_{1g}$ levels. Thus, a parameter value of $\tau_\xi=\tau_\eta=0.992$ can reproduce a level spacing of ~200 cm^{-1} for ^2E_g determined from experiment.

The variation of level differences with the π-expansion parameter $\tau(=\tau_\xi=\tau_\eta)$ as demonstrated in Fig. 7 can be estimated also from the diagonal elements of the LF perturbation matrix of tetragonal symmetry given in terms of Racah parameters A, B, and C

$$\begin{aligned}
&^2E_g \text{ splitting} \quad \Delta E(^2B_1\text{-}^2A_1) = 2\tau^2(1-\tau^2)(3B+C)>0,\\
&^2T_{1g}\text{-}^2E_g \text{ separation} \quad \Delta E(^2A_2\text{-}^2A_1) = 0,\\
&^2T_{1g} \text{ splitting} \quad \Delta E(^2A_2\text{-}^2E) = (-0.5\tau^4+\tau^2-0.5)A\\
&\qquad\qquad + (2.5\tau^4\text{-}0.5\tau^2-2)B + 1.5(\tau^2-1)C<0,\\
&^4A_{2g} \text{ (ground state) splitting} \quad \Delta E(\Gamma_6\text{-}\Gamma_7) = 0.
\end{aligned} \tag{5}$$

It is seen that for $\tau<1$ the ^2E_g level splitting is increased, the $^2T_{1g}$–^2E_g spacing and ground state splitting remain unchanged but the $^2T_{1g}$ splitting tends to be smaller than calculated from conventional LF theory (cf. Eq. 1). The appearence of the A-parameter in the expression for the $^2T_{1g}$ splitting in Eq. 5, which in the spherically symmetric model cancels for any of the transition energies, does not cause difficulties: since its contribution to $\Delta E(^2A_2\text{–}^2E)$ is relatively small due to its coefficient dependent on τ even for large values of A the qualitative aspects of the results will not be changed.

As seen from the full LF calculation (Fig. 7) the total energy separation $\Delta E(^2A_2\text{–}^2A_1)$ is changed only slightly with varying τ which agrees with the observed positions of band C being at constant energy difference compared to A (~600 cm^{-1}) for all compounds considered as well as for the hexaammine complex.[7] Due to the avoided crossing of Γ_6 levels arising from $^2A_2$ and ^2E these states are strongly intermixed at $\tau<0.995$ by which the transition giving rise to band C should obtain an increased $^4B_1 \rightarrow {}^2E$ character. The situation is further complicated by a possible occurrence of a pseudo Jahn–Teller effect in the ^2E state[40] shifting the zero phonon transitions by virtue of vibronic coupling which has not been considered in the present model. A final decision on the assignment of band C can only be made on the basis of more detailed theoretical investigations.

Concerning the ground state $^4A_{2g}$, symmetry adapted expansion coefficients will not be able to calculate increased values for the splitting of this level since both Kramers doublets resulting from spin-orbit interaction have essentially identical orbital wave functions which hardly are affected differently by neighboring atoms that could lead to unequal energies. The large splittings for metal compounds with heavier halogen ligands observed from ESR spectra,[22–24] therefore, are only explained by a relativistic nephelauxetic effect which is described within the framework of LCAO theory in a similar way as Stevens expansion coefficients which allow the spin-orbit coupling parameters to be increased up to values higher than obtained for the free ions.[22,37]

Luminescence Intensity Analysis. The molecular structure of excited electronic states can be determined if in the vibronic spectrum at least partially resolved band profiles are obtained. For an analysis, the relative band intensities in the progression, e.g., of an emission spectrum

$$\nu_n = \nu_{\mathrm{OO}} - \nu_{\mathrm{pr}} - n\cdot\nu_{\mathrm{ac}} \qquad (6)$$

are used where ν_{OO} represents the zero phonon band gap, ν_{pr} a promoting mode which makes the transition electric dipole allowed, and ν_{ac} denotes the accepting mode forming the actual series of equally spaced band peaks.[41] If the pure electronic (zero phonon) transition is allowed, in general, some normal modes of given symmetry (which are totally symmetric if Jahn–Teller effects are absent) may act as promoting and accepting mode as well, a situation which leads to a rather complicated theoretical description of relative transition probabilities. In the Herzberg–Teller coupling scheme of electron–nuclear interaction the vibronic transition moment for g→a is expressed by

$$M^{ga} \approx \langle M_e^{ga} \rangle \langle \chi_v | \chi_{v'} \rangle + \sum_k \frac{\langle M_e^{gk} \rangle}{E_e^a - E_e^k} \sum_\mu \left\langle \left| \frac{\partial H_e}{\partial Q_\mu} \right|^{ka} \right\rangle \langle \chi_v | Q_\mu | \chi_{v'} \rangle + \cdots \qquad (7)$$

where χ_v and $\chi_{v'}$ are total nuclear wave functions of the molecule in the ground and excited state, respectively, $\frac{\partial H_e}{\partial Q_\mu} Q_\mu$ is the linear vibronic coupling operator and E_e^k the energy of the wave function mixing into the states considered.[42] Due to the lack of appropriate electronic wave functions the size of these integrals are not known. Therefore relative Franck–Condon factors can only be compared to the spectra if some of the terms of Eq. 7 can be neglected, i.e., either the first contribution is zero if the pure electronic transition is strictly forbidden or χ_v refers to the zero phonon excitation and $\chi_{v'}$ belongs to a nontotally symmetric representation or the second and all higher terms are vanishingly small compared to the first term in the case of an allowed transition.

In the emission spectra of [X] complexes, apart from side bands assigned to fundamental vibrations, we can identify intensive transitions in combination with the Cr–halogen stretching vibration $\nu_5(a_1)$ as well as progressions in the same mode. Figure 8 depicts the luminescence spectrum of the [Cl]Cl$_2$ complex doped into the corresponding Rh(III) compound. This

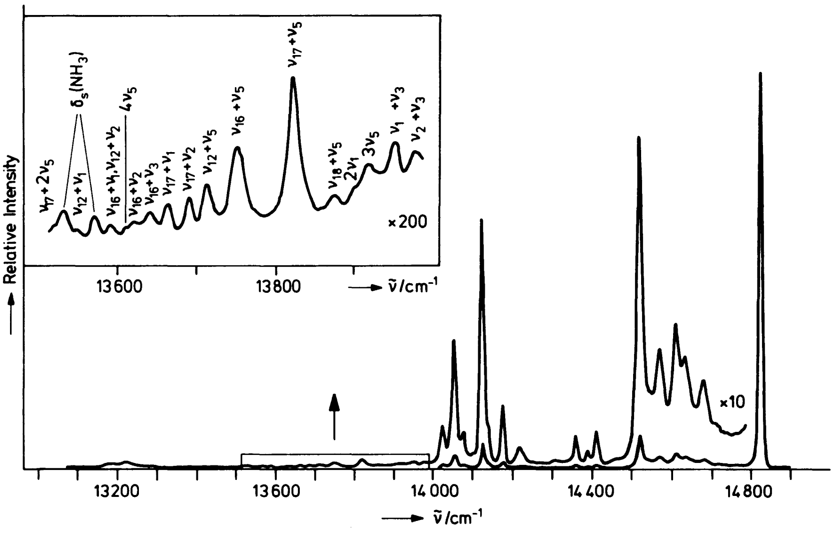

Fig. 8. ^2E_g emission spectrum of Cr^{3+} doped in [Rh(NH$_3$)$_5$Cl]Cl$_2$ at 5 K exhibiting low intensity members in the vibrational progression ($\lambda_{\mathrm{exc}}=514.5$ nm).

Table 3. Intensity Relations in Vibrational Progressions and Nuclear Equilibrium Distortions in the First Excited State

X	σ_X/cm^{-1}	ν_5/ν_{00}	$2\nu_5/\nu_5$	$(\nu_{pr}{}^{a)}+\nu_5)/(\nu_{pr})$	ΔR(Cr–X)/pm
F	7400	0.11	0.12	0.08	≈ 3
Cl	5500	0.086$^{b)}$	0.050$^{b)}$	0.029$^{b)}$	≈ 2
Br	5000	0.118$^{b)}$	0.054$^{b)}$	0.044$^{b)}$	$\leq 1.5^{c)}$
I	4500	0.12	0.06	0.07	$\leq 1.5^{c)}$

a) $\nu_{pr}=\nu_{16}$ or ν_{17}, i.e. δ(Cr–N–H) of e-symmetry. b) Obtained from doped compounds (Rh-host). c) σ(Cr–X) is strongly mixed with the totally symmetric bending mode δ(N–Cr–N).

system has been chosen since intensity relations differing up to four orders of magnitude (1:10^4) could be determined in this case. Some of the intensity relations obtained are compiled in Table 3. Since ν_5 is at the same time promoting and accepting mode, the different numbers calculated for the two progressions considered are explained by the result of the discussion following Eq. 7. For a Franck–Condon analysis, therefore only the intensity relations in the ν_5-progression in combination with the nontotally symmetric vibrational modes δ(Cr–N–H), i.e. ν_{16} and ν_{17}, are evaluated since in these cases the first term in Eq. 7 vanishes for symmetry reasons. The fitting of experimental band intensities in the progression to a theoretical band profile function allows an intramolecular distribution function $I(n,\Delta,\beta)$ to be determined from which the parameter Δ is calculated containing the geometric distortion coordinates in the excited state.[43] The frequency factor $\beta=\nu_g/\nu_a$ is approximately unity since vibrational frequencies ν_a measured from the absorption spectra are almost equal to corresponding values ν_g obtained from IR and Raman data applying to the ground state.

Due to the rapidly decaying band intensities in the progression which moreover is obscured by many other vibrational side bands, a Franck–Condon analysis of the absorption spectrum cannot be carried out. On the other hand are emission spectra by far less perturbed by superpositions since transitions from only one or two of the lowest excited electronic states are involved; therefore they are more appropriate for these analyses. In the present spectra of halogenopentaammines, including the [F] compound, the most intense progressions are found to be due to the $\nu_5(a_1)$ mode which for [F] and [Cl] is an almost pure metal-halogen stretching vibration, but for [Br] and [I] it is appreciably mixed with the $\nu_6(a_1)$ bending mode (cf. Table 1).[33] As indicated in Table 3 the degree of the excited potential curve shift ΔR(Cr–X) proceeds with the size of the σ-antibonding parameter σ_X of the halogen ligand which is to be expected due the increased geometric distortion if the d_{z^2}-orbital (the hetero atom is located on the z-axis) is partially occupied on excitation.

From the distinctly longer progression observed in the $^2E(^2T_{2g})$ absorption spectrum (see Fig. 5) it can be concluded that this state exhibits a larger geometric distortion due to the intermixing of higher energy levels belonging to electron configurations which involve e_g orbitals. Actual numbers cannot be given since normal coordinates for the excited state would be required.

Conclusions

Since for many of the most common complex compounds, as the present halogenopentaammines of chromium(III), the electronic and vibrational energy level schemes are not known in detail, it is recommended to look more closely into well resolved vibronic spectra, i.e. to record low temperature crystalline absorption and emission spectra at high sensitivity. The measured band patterns are strongly dependent on the geometric properties of the crystals, possibly yielding in some instances more detailed information on local distortions than can be obtained from common X-ray investigations. In addition the analysis of the vibronic side bands, if vibrational fine structure is sufficiently well resolved, allows the geometry of some of the excited states to be determined which contributes for characterizing the emitting states being important for explaining photochemical processes.

Conventional ligand field and angular overlap calculations are very useful for carrying out band assignments but they are not in all cases appropriate models for reproducing values of energy levels derived from the experiment. However, small extension or variation of these models, e.g. as presently including symmetry restricted π-orbital expansion factors into the electron repulsion part, may lead to a satisfactory description of experimental results. It is these possible extensions of the model which should be considered in the near future in order to obtain a theory which is generally applicable to a larger variety of cases.

The authors are grateful to Dr. M. A. Atanasov, Sofia, for making us aware of the large level splittings due to orbital expansion factors, to Dr. T. Woike, Jülich, for recording the Raman spectrum, to Prof. R. Kniep and Mr. R. Seidel, Düsseldorf, for carrying out the X-ray investigations. We also appreciate the aid of

Degussa Company, Hanau, supplying us with the rhodium material.

References

1) A. E. Becquerel, "La lumière, ses causes et ses effects," Gauthier-Villars, Paris (1867).

2) Y. Tanabe and S. Sugano, *J. Phys. Soc. Jpn.*, **9**, 753, 766 (1954).

3) J. C. Walling, H. P. Jenssen, R. C. Morris, E. W. O'Dell, and O. G. Peterson, *Opt. Lett.*, **4**, 182 (1979).

4) R. Reisfeld and C. K. Jørgensen, *Struct. and Bondg.*, **49**, 1 (1982).

5) L. J. Andrews, G. H. Beall, and A. Lempicki, *J. Lumin.*, **36**, 65 (1986).

6) A. Ceulemans, M. Dendoven, and L. G. Vanquickenborne, *Inorg. Chem.*, **24**, 1153 (1985).

7) A. Urushiyama, T. Schönherr, and H.-H. Schmidtke, *Ber. Bunsenges. Phys. Chem.*, **90**, 1195 (1986).

8) V. Balzani and V. Carassiti, "Photochemistry of Coordination Compounds," Academic Press, London (1970).

9) "Concepts in Inorganic Photochemistry," ed by E. Zinato and A. W. Adamson, Wiley, New York (1975).

10) H. L. Schläfer, *Z. Chem.*, **10**, 9 (1970).

11) M. Wrighton, H. B. Gray, and G. S. Hammond, *Mol. Photochem.*, **5**, 165 (1973).

12) L. G. Vanquickenborne and A. Ceulemans, *Coord. Chem. Rev.*, **48**, 157 (1983).

13) A. D. Kirk, S. Arunachalam, and D. Kneeland, *Inorg. Chem.*, **25**, 3551 (1986).

14) L. S. Forster, J. V. Rund, and A. F. Fucaloro, *J. Phys. Chem.*, **88**, 5012 (1984).

15) A. F. Fucaloro, L. S. Forster, S. G. Glover, and A. D. Kirk, *Inorg. Chem.*, **24**, 4242 (1985).

16) P. E. Hoggard in "Proc. 7th International Symposium on the Photochemistry and Photophysics of Coordination Compounds," Springer Verlag, Heidelberg (1987) in press.

17) L. S. Forster and O. Monstedt, *J. Chem. Phys.*, **90**, 5131 (1986).

18) C. D. Flint and A. P. Matthews, *J. Chem. Soc., Faraday Trans. 2*, **69**, 419 (1973).

19) S. Decurtins, H. U. Güdel, and K. Neuenschwander, *Inorg. Chem.*, **16**, 796 (1977).

20) T. Schönherr and H.-H. Schmidtke, *Inorg. Chem.*, **18**, 2726 (1979).

21) P. E. Hoggard, *Coord. Chem. Rev.*, **70**, 85 (1986).

22) E. Pedersen and S. Kallesoe, *Inorg. Chem.*, **14**, 85 (1975).

23) T. Schönherr, G. Eyring, and R. Linder, *Z. Naturforsch., a*, **38**, 736 (1983).

24) A. Hauser, M. Mäder, W. T. Robinson, R. Murugesan, and J. Ferguson, *Inorg. Chem.*, **26**, 1331 (1987).

25) Gmelin, "Handbuch der Anorganischen Chemie," Vol. 52, Part C, 8 ed, Verlag Chemie, Weinheim (1965).

26) S. N. Anderson and F. Basolo, *Inorg. Synth.*, **7**, 214 (1963).

27) U. Teutsch and H.-H. Schmidtke, *J. Chem. Phys.*, **84**, 6034 (1986).

28) T. Woike, KFA Jülich, private communication.

29) C. D. Flint and A. P. Matthews, *J. Chem. Soc., Faraday Trans. 2*, **1974**, 1307.

30) T. W. Hambley and P. A. Lay, *Inorg. Chem.*, **25**, 4553 (1986).

31) W. T. M. Andriessen and J. Meuldijk, *Inorg. Chem.*, **15**, 2044 (1976).

32) B. B. Garrett, M. T. Holbrook, and J. A. Stanko, *Inorg. Chem.*, **16**, 1159 (1977).

33) H.-H. Schmidtke and M. Rosner, to be published.

34) H. van den Boom, A. J. J. van Dijsseldonk, and J. C. M. Henning, *J. Chem. Phys.*, **66**, 2368 (1977).

35) L. Dubicki and P. Day, *Inorg. Chem.*, **10**, 2043 (1971).

36) P. E. Hoggard, *Z. Naturforsch., a*, **36**, 1276 (1981).

37) C. K. Jørgensen, *Struct. and Bondg.*, **1**, 3 (1966).

38) J. C. Eisenstein, *J. Chem. Phys.*, **34**, 1628 (1961).

39) W. M. Wallace and P. E. Hoggard, *Inorg. Chem.*, **22**, 491 (1983).

40) A. Ceulemans, N. Bongaerts, and L. G. Vanquickenborne, *Inorg. Chem.*, **26**, 1566 (1987).

41) K. Hakamata, A. Urushiyama, J. Degen, H. Kupka, and H.-H. Schmidtke, *Inorg. Chem.*, **22**, 3519 (1983).

42) H.-H. Schmidtke, "Quantenchemie," VCH-Verlag, Weinheim (1987), p. 277.

43) R. Wernicke, H. Kupka, W. Enßlin, and H.-H. Schmidtke, *Chem. Phys.*, **47**, 235 (1980).